A Synchronization Technique for
Transmissions of Utilizing 4-ary Elliptical Phase Shift Keying

Chunyi Song
Global Information and Telecommunication Institute, Waseda University, Japan
song@aoni.waseda.jp

Shigeru Shimamoto
Graduate School of Global Information and Telecommunication Studies, Waseda University, Japan
shima@waseda.jp

Abstract

Based on assumption of perfect synchronization, a scheme defined as 4-ary Elliptical Phase Shift Keying (4-EPSK) has shown advantage over QPSK on noise performance. However, the analysis also shows that performance of 4-EPSK is vulnerable to synchronization errors. To realize efficient signal detection and simplicity of receiver, in this paper, we propose a timing recovery algorithm for 4-EPSK transmission by employing envelope characteristics of 4-EPSK signal. The proposed technique realizes estimation and recovery of time offset through self-processing envelope of the received signal. The evaluation results demonstrate that the proposed technique is effective when time offset of a received 4-EPSK signal is smaller than half symbol duration.

1. Introduction

Amplitude, phase and frequency of a sinusoid signal are three main modulation variables employed in conventional modulation schemes. In our previous works [1]-[3], modulation schemes employing elliptical carrier signals are generally defined as Elliptical Modulations. Elliptical Modulations introduce new modulation variables compared to conventional modulations. According to analysis results, introduction of new modulation variables provides Elliptical Modulations with higher adaptability to various demands of communication systems than conventional modulation schemes.

A scheme defined as 4-ary Elliptical Phase Shift Keying (4-EPSK) has been proposed and evaluated through simulations in [2] and theoretically analysed in [3]. According to evaluations in [2] and [3], based on assumption of perfect synchronization, 4-EPSK outperforms QPSK at the expense of reducing bandwidth efficiency; in particular, 4-EPSK can dynamically make tradeoffs between power efficiency and bandwidth efficiency by varying eccentricities. This characteristic provides 4-EPSK with adaptability to modern communication systems, which might have various QoS demands with respect to both bandwidth efficiency and power efficiency. However, to achieve efficient and stable performance, [2] supposed to detect signals based on the signal component with peak envelope in one symbol duration. Such detection has strict requirement of synchronization accuracy. Thus, the achieved efficient performance in both [2] and [3] is vulnerable to synchronization error.

Synchronization is of great importance for all digital communication systems. A variety of techniques suitable for PSK transmissions have been developed in some literatures, such as [4]-[8]. Other than constant envelope of PSK signals, 4-EPSK signals have variable envelopes in one symbol duration. By employing the characteristics of envelope variation, we aim to develop an efficient timing recovery technique for 4-EPSK transmission in this paper.

Rest of the paper is organized as follows. Signal characteristics of 4-EPSK are analyzed in Sect.2; a synchronization technique is proposed by exploiting envelope characteristics of 4-EPSK signal in Sect.3; the proposed technique is evaluated through simulations in Sect.4; finally the paper is concluded in Sect.5.

2. Signal Characteristics

2.1. Signal Expression

General expressions of M-EPSK signals are given by

$$
\begin{aligned}
s(t) &= a \cdot R(t, e_c, \varphi_j) \cos(\omega_c t + \alpha_i + \varphi_j) \\
&= a \cdot R(t, e_c, \varphi_j) \cos(\omega_c t + \theta_k)
\end{aligned}
\quad , \tag{1}
$$

as shown in Fig.1, a is semi-major axis, which also denotes signal amplitude; e_c is eccentricity, α_i is offset inclination angle of an ellipse, φ_j is phase defined based on major-axis of the ellipse and we call it major-axis-based phase; θ_k is signal phase and $\theta_k = \alpha_i + \varphi_j$ (i, j and k are integers); $R(t, e_c, \varphi_j)$ is an elliptical radius normalized by semi-major axis and given by

$$
R(t, e_c, \varphi_j) = \sqrt{\frac{1 - e_c^2}{1 - e_c^2 \cos^2(\omega_r t + \varphi_j)}} \quad , \tag{2}
$$

where ω_r is revolution angular frequency of elliptical radius, and the elliptical signals used in this paper are generated by setting same value for ω_r and carrier angular frequency ω_c.

To emphasize the difference of carrier signals, we express signal constellation of QPSK based on a circle and signal constellation of 4-EPSK based on ellipses [2]. Then as shown in Fig.2, φ_j is equal to either of 0 and π, and (2) is simplified to

$$
R(t, e_c) = \sqrt{\frac{1 - e_c^2}{1 - e_c^2 \cos^2(\omega_r t)}} \quad . \tag{3}
$$

Consequently, (1) can be simplified to

$$
\begin{aligned}
s(t) &= a \cdot R(t, e_c) \cos(\omega_c t + \theta_k) \\
&= a_I \cdot \underbrace{R(t, e_c) \cdot \cos \omega_c t}_{C_{EI}} - a_Q \cdot \underbrace{R(t, e_c) \cdot \sin \omega_c t}_{C_{EQ}}
\end{aligned}
\quad , \tag{4}
$$

where a_I and a_Q are amplitudes of in-phase and quadrature phase components, respectively; from Fig.2, we have $\theta_k = \alpha_i$ or $\theta_k = \alpha_i + \pi$; orthogonal signals of C_{EI} and C_{EQ} denote transmission carriers in I-channel and Q-channel respectively. By substituting $\theta_k = (2k-1)\pi/4$ ($k=1,2,3,4$) to (4), we achieve same expression with 4-EPSK signals derived in [2] and [3].

2.2. Characteristics of Signal Envelope

From (4), we have

$$S_I(t) = a_I \cdot R(t,e_c) \cdot \cos \omega_c t$$

$$S_Q(t) = a_Q \cdot R(t,e_c) \cdot \sin \omega_c t \quad , \tag{5}$$

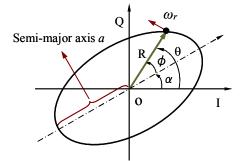here S_I and S_Q denote signals transmitted in I-channel and Q-channel, respectively.

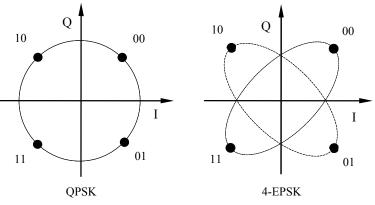**Figure 1. Definitions of variables in an elliptical signal**

Figure 2. Signal constellations of QPSK and 4-EPSK

Then signal envelope of 4-EPSK can be derived as

$$\gamma = \sqrt{[s_I(t)]^2 + [s_Q(t)]^2}$$

$$= \sqrt{[a_I \cdot R(t,e_c) \cdot \cos \omega_c t]^2 + [a_Q \cdot R(t,e_c) \cdot \sin \omega_c t]^2}$$

$$= \sqrt{\frac{1}{2} a^2 [R(t,e_c)]^2} = \frac{\sqrt{2}a}{2} R(t,e_c) \quad , \tag{6}$$

where semi-major axis a is a constant, so characteristics of envelope are decided by $R(t,e_c)$. From (3) we know that $R(t,e_c)$ changes nonlinearly according to values of e_c and t. As instances, we demonstrate in Fig.3 variation of the envelope in a symbol duration, by setting eccentricity to 0.3, 0.6 and 0.9, respectively. The results confirm that envelope variation

becomes more evident with the increase of eccentricity, and show that if we define the same value for cycle duration and symbol duration, then duration of envelope variation equals to half symbol duration.

Other than variable amplitudes of in-phase and quadrature phase components in 8-EPSK signals, 4-EPSK signals have same amplitude of in-phase and quadrature phase components [2]. As shown in (6), this provides the simplicity in obtaining signal envelope. By employing the characteristic of envelope variation, we propose a timing recovery algorithm for 4-EPSK transmission in subsequent sections.
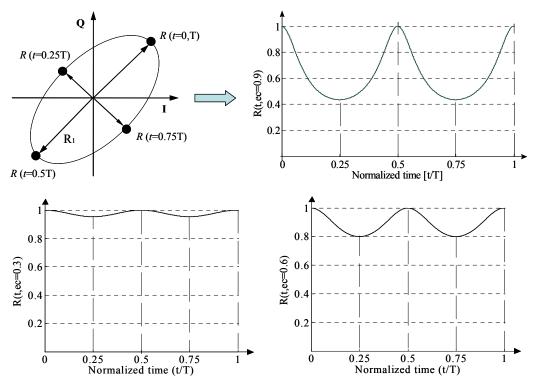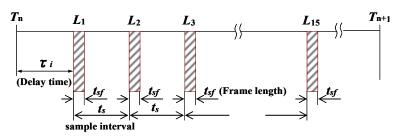

Figure 3. Envelope variation in a symbol duration

3. Proposition of synchronization technique for 4-EPSK Transmission

3.1. Optimum number of sample frame

We show in Fig.4 the way to obtain sample frames of envelope based on delay of arrived signals, where: (1) term τ_i denotes delay time of received signal; N sample frames are defined within half symbol duration, with same frame length (t_{fl}) and same sampling interval (t_s); an envelope of sample frame denoted by L_i (i=1,2,…N) is average envelope of each sample frame.

In 4-EPSK, if we define that one cycle length equals to a symbol duration, then duration of envelope variation is equal to half symbol duration. So once assuming delay time τ_i to be smaller than half symbol duration, i.e. $\tau_i \leq T/2$, combination of $L_1 \sim L_N$ calculated based on any fixed value of τ_i is unique. Thus, we can extract information of time shift from characteristics of combinations of $L_1 \sim L_N$. This is the basic idea behind the proposition in this paper.

Figure 4. Sampling of envelope

From Fig.3 and Fig.4 we know that number of sample frame is inversely proportional to sampling interval t_s within half symbol duration. If we set the number to a small value, t_s becomes large and L_i (i=1,2…N) becomes more distinctive to each other. Combination of distinctive L_i will contribute to estimation accuracy of delay time; however, based on small number of sample frames, the synchronization accuracy becomes more sensitive to the improper detection of L_i, and so it easily leads to unstable performance. If we set number of sample frame to a large value, similar conflicting results will be achieved. Therefore, a value that can realize optimal performance must exist. We investigate synchronization performance by setting number of sample frame from 7~21, and achieve the best performance when number of sample frame equals to 15. We then roughly define 15 as the optimum number.

3.2. Estimation of time offset

To simplify the explanation, we assume that delay time τ_i is smaller than $T/4$ when illustrating mathematic model of the timing recovery technique.

By equally dividing assumed range of delay, i.e. [0, $T/4$], into eight sub ranges, the achieved sub ranges are defined as time frames and denoted by Tf_m (m=1,2,…8). Each time frame is further divided into a certain number of small time ranges and which are called time slots here. In this work, estimation of τ_i is accomplished through following two steps: 1) identify the time frame Tf_i that τ_i lies in; 2) decide the time slot that τ_i lies in.

Among eight values of L_i (i=2k+1, k=0,1,…7), let L_{max} and L_{Smax} denote the largest value and second largest value respectively, we found that combination of L_{max} and L_{Smax} corresponding to each time frame is unique. The one-to-one correspondence relation is shown in Table 1. Accordingly, by calculating the combination of L_{max} and L_{Smax}, we can work out the time frame that delay time τ_i lies in.

To further identify the time slots that τ_i lies in, we define K_n (n=1,2,…8) as the decision factor of time slots in time frame Tf_i. Expressions of decision factors are decided based on both time frame and eccentricity. Once eccentricity is fixed, each time frame corresponds to a unique expression of decision factor. As an instance, we show here the decision factors that are defined for 4-EPSK with eccentricity of 0.9 as

$$Tf_1: K_1 = [L(14)+L(15)]/[L(1)+L(2)+L(3)] \qquad Tf_2: K_2 = [L(1)+L(2)]/[L(13)+L(14)+L(15)]$$

$$Tf_3: K_3 = [L(1)+L(15)]/[L(12)+L(13)+L(14)] \qquad Tf_4: K_4 = [L(14)+L(15)]/[L(11)+L(12)+L(13)]$$

$$Tf_5: K_5 = [L(11)+L(12)]/[L(13)+L(14)+L(15)] \qquad Tf_6: K_6 = [L(10)+L(11)]/[L(12)+L(13)+L(14)] \quad (7)$$

$$Tf_7: K_7 = [L(9)+L(10)]/[L(11)+L(12)+L(13)] \qquad Tf_8: K_8 = [L(8)+L(9)]/[L(10)+L(11)+L(12)]$$

To achieve optimum results, L_i used in (7) are selected according to following two rules: 1) L_i of large values are selected since they have better noise immunity; 2) in the same time

frame, if frame lengths that keep increasing are used in numerator, then frame lengths that keep decreasing are selected for denominator, vice versa. Through this way, decision factors that are most sensitive to value change of L_i are defined, which contributes toward improving the estimation accuracy of delay.

Fig.5 shows an example of configuration of time slots within one time frame. τ_{0_N} is the center value of Ts_N. Assuming that time delay of received signal τ_i is judged in time frame Tf_i, we then can work out the time slot that τ_i lies in by calculating the associated decision factor K_i and estimate the delay time to be τ_{0_i}. Consequently, receiver clock needs to be adjusted backward with τ_{0_i} and the adjustment is mathematically expressed as

$$\tau_{r\_i} = \tau_i - \tau_{0\_i} \quad , \tag{8}$$

where τ_{r_i} stands for recovered time offset.

In (8), τ_{0_i} is the center value of time slot Ts_i, so τ_{r_i} is highly possible to be a negative value. Negative value of τ_{r_i} means that the receiver clock will be excessively adjusted and which then leads to error synchronization. To solve this problem, based on (8), we adjust the receiver clock forward with $T/2$ before carrying out demodulations. The execution is mathematically expressed as

$$\tau_{r\_i} = \tau_i - \tau_{0\_i} + T/2 \quad . \tag{9}$$

To recover this additional adjustment of receiver clock, we conduct a modified logic processing in 4-EPSK demodulator when employing the proposed timing recovery technique. Based on Gray code bit mapping defined in Fig.2, data bits are phase-modulated according to: $[00]{\rightarrow}[\pi/4]$, $[10]{\rightarrow}[3\pi/4]$, $[11]{\rightarrow}[5\pi/4]$ and $[01]{\rightarrow}[7\pi/4]$. Time-shift of $T/2$ in (9) is equivalent to phase-shift of π, so the logic in demodulator should change to: $[5\pi/4]{\rightarrow}[00]$, $[7\pi/4]{\rightarrow}[10]$, $[\pi/4]{\rightarrow}[11]$ and $[3\pi/4]{\rightarrow}[01]$.

We summarize above process and show in Fig.6 the flow chart of estimating and recovering a time delay τ_i when assuming it is smaller than $T/4$. In the case when we need to repeatedly execute the algorithm, instead of random generated τ_i used in the first execution, τ_{r_i} achieved in (9) will be applied to calculate values of $L_1{\sim}L_{15}$ in the subsequent executions. When limitation of τ_i is extended to $T/2$, more time frames, and accordingly more decision factors of time slots, need to be defined and calculated in the proposed technique.

According to above demonstration and analysis, frame length t_{fl}, sampling interval t_s and sample number in one sample frame sn can substantially influence the timing recovery accuracy. We define these three parameters as influence factors.

Table 1. One-to-one correspondence between time frame and combination of largest two frame lengths

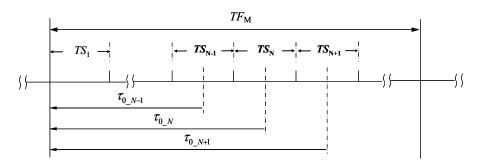| Time Frames	TF_1	TF_2	TF_3	TF_4	TF_5	TF_6	TF_7	TF_8
L_{max}	L_1	L_{15}	L_{15}	L_{13}	L_{13}	L_{11}	L_{11}	L_9
L_{Smax}	L_{15}	L_1	L_{13}	L_{15}	L_{11}	L_{13}	L_9	L_{11}

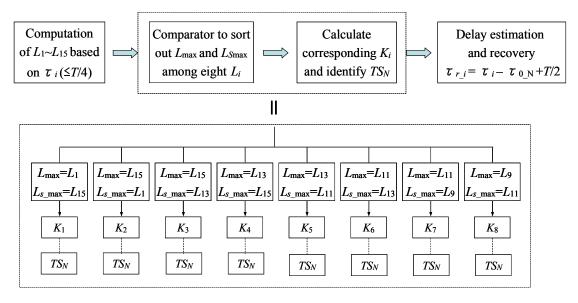Figure 5. Estimation of delay based on definitions of time slots

Figure 6. Flow chart of estimation and recovery process

4. Evaluation of the proposed synchronization technique

4.1. Influence on error performance of 4-EPSK

Since the proposed synchronization technique is only effective when delay time τ_i is smaller than $T/2$, we assume that τ_i is smaller than $T/2$ in the evaluations. Features of envelope demonstrated in Fig.3 reveal that only when eccentricity is set a large value, it is necessary and meaningful to apply the proposed synchronization algorithm in detection of 4-EPSK signals. Based on such consideration, we apply the proposed algorithm to 4-EPSK with eccentricities of 0.8 and 0.9 respectively. For description simplicity, they are denoted by 4-EPSK_0.8 and 4-EPSK_0.9 respectively in rest part of the paper.

We define B_nT to be 1.17, a value that is same with the setting in [2]; in further, according to above investigation results, we set sn=80 for 4-EPSK_0.9 and sn=100 for 4-EPSK_0.8, and set frame length to be $t_{fl}=T/64$ and sampling interval to be $t_s=T/32$ for both cases. Then based on 1,000,000 symbol signals and under AWGN channel, we calculate and compare the error probabilities of 4-EPSK achieved by employing the proposed timing recovery technique and by assuming perfect synchronization. The results are demonstrated in Fig.7 and show that

very close performance is achieved in both cases. Therefore, the proposed synchronization technique is effective based on assumed simulation condition. Here, influence of processing time in timing recovery to the demodulation results has not been taken into account.

4.2. Distribution of recovered time offset

To get insight into accuracy of the proposed timing recovery technique, we also investigate distribution of recovered time offset based on predefined three ranges, which are $[0, T/128]$, $[0, T/64]$ and $[0, 5T/256]$. In the signal detection method proposed in [2], synchronization error leads to reduction of signal-to-noise ratio (SNR). As reference, reduction of SNR equivalent to above three predefined threshold values of time offset are calculated and summarized in Table 2.
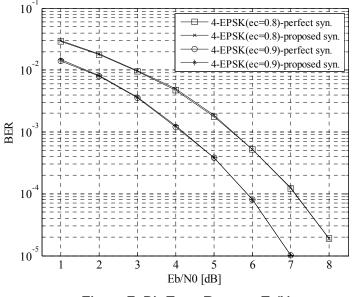

Figure 7. Bit-Error-Rate vs. E_b/N_0

Fig.8 shows the distribution of recovered time offset for 4-EPSK_0.8 and 4-EPSK_0.9, respectively. For 4-EPSK_0.8, around 62% of the recovered time offset are smaller than $T/128$ when E_b/N_0=1dB, and the probability exceeds 90% when E_b/N_0=7dB; more than 90% of the recovered time offset are smaller than $T/64$ when E_b/N_0=1dB, and the probability reaches 100% when E_b/N_0=9dB; around 96% of the recovered time offset are smaller than $5T/256$ when E_b/N_0=1dB, and the probability reaches 100% when E_b/N_0=7dB. For 4-EPSK_0.9, around 82% of the recovered time offset are smaller than $T/128$ when E_b/N_0=1dB, and this probability exceeds 90% when E_b/N_0 is larger than 3dB; more than 99% of the recovered time offset are smaller than $T/64$ when E_b/N_0=1dB, and this probability reaches 100% when E_b/N_0=6dB; around 99.8% of the recovered time offset are smaller than $5T/256$ when E_b/N_0=1dB, and this probability reaches 100% when E_b/N_0=5dB.

We notice that time offset larger than $5T/256$ still exist in Fig.8. To improve recovery accuracy, we may take either of following two measures: set three influence factors to optimum values or repeat the timing recovery process. Here, we investigate the effectiveness of latter measure.

We execute the timing recovery algorithm twice by defining the recovered time offset achieved from first execution as the initial delay time for second execution. The final results are summarized in Fig.9. Compared to the results in Fig.8, recovery accuracy has been significantly improved. In Fig.9, more than 99.99% of the recovered time offset are smaller than $5T/256$ when E_b/N_0=1dB, and the probability stably reaches 100% when E_b/N_0 is increased to 3dB. Since the second execution is completely same with the first execution, the performance improvement is realized without heavily increasing complexity. Such a characteristic is very attractive especially when 4-EPSK is suffering low signal-to-noise ratio.

We also find that based on the assumed simulation condition, after the second execution of the algorithm, further repeated executions do not contribute toward apparent performance improvement. Therefore, in a practical implementation, optimal execution times should be decided according to exact communication condition.

Table 2. Reduction of SNR equivalent to threshold values of time offset

Time offset		$T/128$	$T/64$	$5T/256$
e_c=0.9	$\Delta\gamma$ [dB]	0.0443	0.1743	0.2689
e_c=0.8	$\Delta\gamma$ [dB]	0.0185	0.0736	0.1142

(*a*) Implementation in 4-EPSK_0.8   (*b*) Implementation in 4-EPSK_0.9
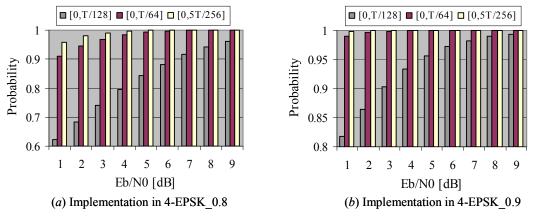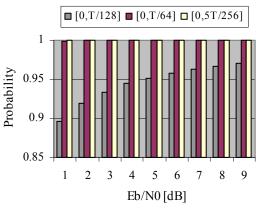
Figure 8. Distribution of recoverred time offset

Figure 9. Distribution of time offset after second-execution of timing recovery process

5. Conclusion

In this work, we propose a nondecision-aided synchronization technique for 4-EPSK transmission, which realize estimation of time offset by employing envelope characteristics of elliptical signals. Evaluation results show that the proposed technique can achieve efficient performance. In particular, recovery accuracy by adopting the proposed technique can be substantially improved by simply repeatedly executing the same recovery process. This characteristic is very attractive and suggests that the proposed algorithm can also work effectively even when 4-EPSK transmission is suffering low signal-to-noise ratio.

4-EPSK signals have same amplitudes of in-phase and quadrature phase components, which provides the simplicity in obtaining signal envelope. In addition, proposed technique realized timing recovery mechanism through self-processing the envelope of received signal. This also strengthens the advantage of simplicity for the proposed algorithm.

The proposed synchronization technique is effective only when delay of the arrived 4-EPSK signal is smaller than half symbol duration.

Acknowledgement

References

[1] Chunyi Song and S.Shimamoto, "Proposal and Evaluation of 8-ary Elliptical Phase Shift Keying". *Proc. IEEE International Conference on Communications* (*ICC*) 2005, Vol.1, Page(s): 598 – 602.

[2] Chunyi Song and S.Shimamoto, "Improvement on Power Efficiency of MPSK by Employing Elliptical Signals". *Proc. of IEEE Wireless Communications and Networking Conference* (*WCNC*) 2006, Vol.4, page(s): 1921- 1926.

[3] Chunyi Song and S.Shimamoto, "Effects of Eccentricity to Performance of M-ary Elliptical Phase Shift Keying (M=4,8)". *Proc. of IEEE WCNC* 2008,page(s):1945-1949.

[4] L. E. Franks, "Carrier Bit Synchronization In Data Communications-A Tutorial Review, " I*EEE Trans. on Comm.*, Vol.28, No.6, Aug. 1980, pp.1107-1120.

[5] E.M.Gardner, "A BPSK/QPSK timing–error detector for sampled data receiver," I*EEE Trans. on Comm.*, Vol.34, No.5, May.1986, pp.423-429.

[6] M.Moeneclaey and T.Natselé "Carrier Independent NDA symbol synchronization for MPSK, operating at only one sample per symbol," *Proc. IEEE Globecom* 90, Vol.1, pp.594-598.

[7] W. G. Cowley and L. P. Sabel, "The Performance of Two Symbol Timing Recovery Algorithms for PSK Demodulators," I*EEE Trans. on Comm.*, Vol.42, No.6, Jun.1994, pp.2345-2355.

[8] Kai Shi and Erchin Serpedin, "Fast Timing Recovery for Linearly and Nonlinearly Modulated Systems," I*EEE Trans. on Veh. Tech.*, Vol.54, No.6, Nov.2005, pp.2017-2023.

Authors

Chunyi SONG received B.E. and M.E. degrees from Jilin University, Jilin, China, in 2000 and 2003, respectively. He was special research student during Oct.2001-Mar.2003 in Graduate School of Global Information and Telecommunication Studies, Waseda University, Tokyo, Japan, supported by Japanese government scholarship. He joined Global Information and Telecommunication Institute (GITI) of Waseda University in April 2007, where he is currently a Research Associate and working toward Ph.D degree. His main research interests include modulation, coding theory, ad hoc network and cognitive radio. He is a member of IEEE and IEICE.

Shigeru SHIMAMOTO received the B. E. and M. E. degrees from the University of Electro-Communications, Tokyo, Japan, in 1985 and 1987, respectively. He received the Ph. D. degree from Tohoku University, Sendai, Japan, in 1992. He joined NEC Corporation from 1987 to 1991. From 1991 to 1992, he was a research associate in the University of Electro-Communications, Tokyo, Japan. He was a research associate in Gunma University, Gunma, Japan, from 1992 to 1993. From 1994 to 2000, he was an associate professor in the Graduate School of Global Information and Telecommunication Studies (GITS), Waseda University, Tokyo, Japan. Since 2001, he has been a professor in the Graduate School of GITS, Waseda University. His main fields of research interests include satellite communications, mobile communications, optical wireless communications, ad-hoc networks, sensor networks, and body area networks. Dr. Shimamoto is a member of the IEEE and IEICE. He is a visiting professor at Stanford University in 2008.